Journal of Dental Research
2023, Vol. 102(4) 459–466

DOI: 10.1177/00220345221146454
journals.sagepub.com/home/jdr

Periderm Fate during Palatogenesis: TGF-β and Periderm Dedifferentiation

G. Saroya[1], J. Hu[1,2], M. Hu[1,2], C. Panaretos[1], J. Mann[1], S. Kim[3], J.O. Bush[3], and V. Kaartinen[1]

Abstract

Failure of palatogenesis results in cleft palate, one of the most common congenital disabilities in humans. During the final phases of palatogenesis, the protective function of the peridermal cell layer must be eliminated for the medial edge epithelia to adhere properly, which is a prerequisite for the successful fusion of the secondary palate. However, a deeper understanding of the role and fate of the periderm in palatal adherence and fusion has been hampered due to a lack of appropriate periderm-specific genetic tools to examine this cell type in vivo. Here we used the cytokeratin-6A (Krt-6a) locus to develop both constitutive (*Krt6ai-Cre*) and inducible (*Krt6ai-Cre^{ERT2}*) periderm-specific Cre driver mouse lines. These novel lines allowed us to achieve both the spatial and temporal control needed to dissect the periderm fate on a cellular resolution during palatogenesis. Our studies suggest that, already before the opposing palatal shelves contact each other, at least some palatal periderm cells start to gradually lose their squamous periderm-like phenotype and dedifferentiate into cuboidal cells, reminiscent of the basal epithelial cells seen in the palatal midline seam. Moreover, we show that transforming growth factor–β (TGF-β) signaling plays a critical periderm-specific role in palatogenesis. Thirty-three percent of embryos lacking a gene encoding the TGF-β type I receptor (*Tgfbr1*) in the periderm display a complete cleft of the secondary palate. Our subsequent experiments demonstrated that *Tgfbr1*-deficient periderm fails to undergo appropriate dedifferentiation. These studies define the periderm cell fate during palatogenesis and reveal a novel, critical role for TGF-β signaling in periderm dedifferentiation, which is a prerequisite for appropriate palatal epithelial adhesion and fusion.

Keywords: cleft palate, cell biology, cell differentiation, growth factor(s), morphogenesis, craniofacial biology/genetics

Introduction

The development of the mammalian secondary palate (palatogenesis) is a complex developmental process that takes place during early embryogenesis (Bush and Jiang 2012; Lan et al. 2015). In palatogenesis, bilateral palatal primordia (palatal shelves) protrude out from the maxillary process of the first pharyngeal arch, grow down along the sides of the tongue, and then rapidly elevate and fuse in the midline. Palatal shelves are covered by the ectoderm-derived epithelium, while the underlying mesenchyme is mostly derived from the neural crest and, to a lesser extent, from the mesoderm. Failure in palatogenesis results in cleft palate, one of the most common congenital birth defects in humans.

During the past decades, studies exploring molecular mechanisms in the palatal mesenchyme and epithelium have unraveled signaling processes and gene regulatory networks that regulate palatal shelf growth, patterning, elevation, and fusion (Bush and Jiang 2012; Lane and Kaartinen 2014; Lan et al. 2015). These studies have exposed significant and unique differences in epithelial–mesenchymal interactions regulating morphogenesis of the anterior palate, which eventually forms the bony hard palate, and of the posterior palate, which contributes to the formation of the muscular soft palate. These discoveries have only been made possible by advances in tissue-specific gene targeting technologies, which have allowed manipulation of genes and development of specific molecular tools. In this context, neural crest–specific Cre driver lines (Wnt1-Cre and P0-Cre), a palatal mesenchyme-specific driver line (Osr2-Cre), and an epithelium-specific driver line (Krt14-Cre) have commonly been used to dissect cell type–specific molecular mechanisms regulating palate development (Chai et al. 2000; Dudas et al. 2006; Xu et al. 2006; Lan et al. 2007; Liu et al. 2012). However, only recently we have started to thoroughly understand the critical role of yet another specific cell type called the periderm (PD) in palatogenesis (Richardson et al. 2014; Hu et al. 2015; Richardson et al. 2017). Before palatal fusion, the

[1]Department of Biologic and Materials Sciences, University of Michigan School of Dentistry, Ann Arbor, MI, USA
[2]College of Literature, Sciences, and the Arts, University of Michigan, Ann Arbor, MI, USA
[3]Department of Cell and Tissue Biology and Program in Craniofacial Biology, University of California San Francisco, San Francisco, CA, USA

A supplemental appendix to this article is available online.

Corresponding Author:
V. Kaartinen, Department of Biologic and Materials Sciences, University of Michigan School of Dentistry, 1011 N. University, Ann Arbor, MI 48109, USA.
Email: vesak@umich.edu

PD functions as a protective layer in the oral cavity, preventing aberrant intraoral adhesions, yet its function has to be eliminated at the sites where the fusion is desired (e.g., the medial edge epithelial [MEE] cells of the secondary palate) (Hammond et al. 2019). Previous studies have presented different possibilities for the cellular fate of the palatal midline PD. It has been suggested that PD cells are sloughed off via a process called desquamation, that they die via programmed cell death, and that they migrate to oral and nasal epithelial triangles (Yoshida et al. 2012; Hu et al. 2015; Richardson et al. 2017). Nevertheless, the lack of appropriate genetic tools has prevented detailed studies on the exact fate of the palatal periderm during palatal epithelial fusion.

Transforming growth factor–β (TGF-β) signaling has been shown to be important for successful palatal shelf growth and fusion both in humans and in animal models (Lidral et al. 1998; Jugessur et al. 2003; Vieira et al. 2003; Xu et al. 2008; Iwata et al. 2013; Parada et al. 2013). The gene encoding TGF-β3 (*Tgfb3*) is specifically expressed in palatal MEE cells (palatal epithelial cells that are destined to form a contact and fuse) (Fitzpatrick et al. 1990; Pelton et al. 1990), and mice deficient in *Tgfb3* display a complete cleft of the secondary palate with 100% penetrance (Kaartinen et al. 1995; Proetzel et al. 1995). Remarkably, epithelium-specific deletion of the genes encoding TGF-β type I or type II receptors with the well-characterized Krt14-Cre driver line (Andl et al. 2004) never results in complete cleft palate. Instead, these mice typically display posterior submucous cleft and anterior palatal hole (i.e., the palatal phenotype in these epithelium-specific TGF-β receptor mutants was consistently less severe than that in the *Tgfb3* germline mutants) (Dudas et al. 2006; Xu et al. 2006). We have previously hypothesized that this discrepancy is likely due to the fact that the Krt14-Cre driver line used in these studies does not recombine in the PD (Lane,Yumoto, Pisano, et al. 2014) (Appendix Fig. 1). In fact, a specific role for TGF-β signaling in the control of the PD fate has previously been suggested by Yoshida et al. (2012) and Hu et al. (2015), who showed that either chemical inhibition of TGF-β type I receptor or genetic abrogation of *Tgfb3* prevented PD desquamation. In contrast, Richardson et al. (2017) suggested that the main role of TGF-β signaling is to suppress p63 expression in the basal cells of the MEE, which allows palatal fusion by facilitating PD migration.

Studies on gene function specifically in the palatal PD during palatogenesis have been limited by the fact that there are no useful PD-specific Cre driver lines currently available. To address this problem, we searched for genes that are specifically expressed in the PD of prefusion palatal shelves and identified cytokeratin-6a (Krt-6a) as a promising candidate. Subsequently, by using the CRISPR-Cas9 gene-editing technology, we generated and validated both *Krt6ai-Cre* and *Krt6ai-Cre^{ERT2}* knockin mouse lines. These lines were used to identify the fate of palatal PD and to examine the PD-specific role of TGF-β signaling during palate fusion.

Materials and Methods

Generation, validation, and characterization of *Krt6aiCre* and *Krt6aiCre^{ERT2}* mouse lines:

To generate *Krt6aiCre* and *Krt6aiCre^{ERT2}* mice, we used CRISPR/Cas9 technology (see Appendix for details). All the candidate founder lines showed correct targeting without any undesired mutations. Two independent founders were used for each line to establish the *Krt6aiCre* and *Krt6aiCre^{ERT2}* mouse lines. They both transmitted to the germline with high efficiency.

Timed matings were set up for *Krt6aiCre* and *Krt6aiCre^{ERT2}* male mice with *Gt(ROSA)26Sor$^{tm4(ACTB-tdTomato,-EGFP)Luo}$*/J (mTmG) (Jackson Strain #:007576) female mice. When applicable, tamoxifen was administered at embryonal day 13.0 (E13.0) (0.20 mg/g body weight [bw], oral gavage), and embryos were harvested at E14.0 to E16.0. The *Tgfbr1*-flox animals have been previously described (Dudas et al. 2006).

This research was conducted in strict accordance with the recommendations in the Guide for the Care and Use of Laboratory Animals of the National Institutes of Health. The study obeys the ARRIVE (Animal Research: Reporting of Vivo Experiments) guidelines. The experiments described here are specifically approved by the Institutional Animal Care and Use Committee at the University of Michigan–Ann Arbor (Protocol Number: PRO00010216). Mouse colonies were maintained in a standard microisolator animal facility. Mice used in this study were maintained in outbred (C57BL/6 × SJL) background. Both male and female embryos (E14.0–E16.0) were included in analyses.

Lineage tracing, Immunohistochemistry, TUNEL Assays, and Fluorescence Microscopy

Harvested embryos were fixed in 4% paraformaldehyde overnight at +4°C, transferred to phosphate-buffered saline (PBS), processed through sucrose gradient to OCT compound, and embedded for frozen sectioning. Sections (10 µm thick) were stained overnight with primary antibodies at +4°C (antibodies: Krt6a, Biolegend 905701; p63, R&D systems AF1916; ZO1, Invitrogen 33-9100; Krt17, Biolegend 697202; Krt14, Covance PRB-155P). Binding of each antibody was visualized with Alexa Fluor 594 and 647 secondary antibodies (ThermoFisher) on slides mounted with ProLong Diamond (with or without DAPI). Apoptotic cells were detected with the Biotium CF-Dye TUNEL assay (30074). Images were acquired using a Nikon Eclipse C1 confocal microscope or Leica DMi8 controlled by Leica Application Suite X, 3.7.4.23463 software. Three or more independent samples were analyzed in each assay.

Histology and DAPI Dilactate Staining

The embryos were harvested in Dulbecco's phosphate-buffered saline, fixed overnight in 4% paraformaldehyde at +4°C, and processed for paraffin embedding. Briefly, the embryos

were dehydrated, oriented, and embedded in fresh Blue Ribbon Tissue Embedding Medium (Leica Surgipath). Serial sections (5 µm thickness) were mounted on Superfrost plus slides (ThermoFisher) and stored at room temperature. Hematoxylin and eosin staining was performed using a standard protocol. The stained sections were viewed and documented using an Olympus BX51 microscope equipped with an Olympus DP71 digital camera. DAPI-dilactate staining was performed as described by Sandell et al. (2018). Stained embryos were photographed using the Leica M165FC epifluorescence stereomicroscope equipped with an Olympus DP73 digital camera and software. Three or more independent samples were analyzed in each assay.

Image Analysis

Nuclear shape assays (length/width ratio) of green fluorescent protein (GFP)–expressing cells were conducted by using Leica AIVIA artificial intelligence–guided image analysis and visualization solutions (AIVIA version 10.0.0). The software was trained to build a model that identified nuclei and measured the nuclear shape (length vs. width). The training model was applied to the control and mutant images (each datapoint represents an independent sample [mouse embryo]). GraphPad Prism version 9.3.1 (GraphPad Software) was used to perform unpaired 2-tailed Student's *t* tests, where *P* values less than 0.05 are considered significant.

Results

Krt6aiCre *Induces Recombination in the PD of the Prefusion Palatal Shelves*

Our preliminary studies indicated that the cytokeratin-6a (Krt6a) protein was specifically located in the PD of prefusion palatal shelves. Upon palatal shelf contact and fusion, Krt6a-positive cells could be seen throughout the midline epithelial seam (Fig. 1).

To develop a PD-specific Cre driver line, we used the *CRISPR*/*Cas9* gene-editing technology to introduce an *iCrepA* cassette in-frame into exon 1 of the *Krt6a* gene (Fig. 2). When crossed with the ROSAmTmG reporter line, we could detect *Krt6ai-Cre*–induced recombination in the outer periderm, nostrils, ear pinnae, and eyelids in embryos harvested at E14.5 (Appendix Fig. 2). In the oral cavity, recombination was detected broadly in the superficial PD cells (Appendix Fig. 3). However, in the sublingual epithelium and superior lingual epithelium, the *Krt6aiCre*-induced recombination could be seen in both the PD and the underlying basal epithelium (Appendix Fig. 3). In elevated prefusion palatal shelves, we could detect *Krt6ai-Cre*–induced recombination specifically in the superficial PD cells, while the p63-positive basal epithelial cells did not show recombination (Fig. 2B, C). Just before the palatal shelves formed a contact with each other, a subset of cells that had undergone the *Krt6aiCre*-induced recombination had lost their flattened phenotype and became more cuboidal (Fig. 2D). This phenotype became very prevalent (>50% of

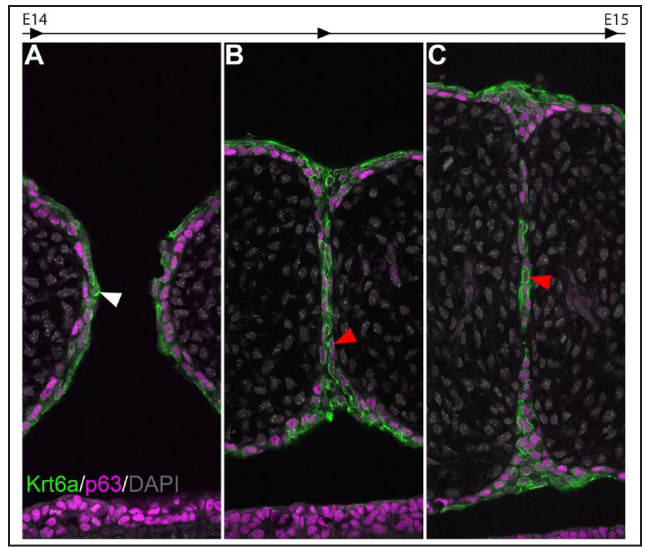

Figure 1. Cytokeratin 6a is specifically expressed in the periderm of prefusion palatal shelves. (**A**) Palatal shelves before contact at E14. (**B**) Palatal midline seam during the early fusion (E14.5). (**C**) Palatal midline seam during the late fusion (E15). Green fluorescence, Krt6a; magenta fluorescence, p63; Counterstaining with DAPI, gray nuclear fluorescence. White arrowheads mark flattened peridermal layer; red arrowheads mark Krt6a-expressing cells during fusion.

recombined cells had lost their flattened squamous phenotype) in the palatal shelves that had formed a contact with each other (Fig. 5B). Simultaneously, the p63-positive basal epithelial cells started to show recombination as well, and as a consequence, most of the cells in the forming midline epithelial seam were recombined by *Krt6aiCre* (Fig. 2F and Appendix Fig. 3D). As expected, cell–cell junctions of the flattened periderm stained positive for the tight junction marker, ZO1, while the cuboidal midline epithelial seam cells showed strong membrane-bound green fluorescence but had lost the positive ZO1 staining (Appendix Fig. 4). In prefusion and contacting palatal shelves, the recombined cells did not show apoptosis, while the midline seam showed characteristic TUNEL staining (Appendix Fig. 5) as reported earlier (Cuervo and Covarrubias 2004). To conclude, dynamics and patterns of *Krt6aiCre*-induced recombination were very similar to those seen in immunostaining for Krt6a, as shown in Figure 1.

Some of the Flattened Periderm Cells May Dedifferentiate to Cuboidal Basal Epithelial-Like Cells during Palatal Fusion

To be able to more accurately define the fate of palatal PD, we developed a tamoxifen-inducible *Krt6aiCre*^{ERT2} mouse line by using the targeting strategy described above (Fig. 3). These mice were crossed with ROSA:mTmG mice, and Cre-mediated recombination in *Krt6aiCre*^{ERT2}*::mTmG* mice was induced by a single dose of intraoral tamoxifen administration at E13.0 (the amount of tamoxifen was titrated so that only a limited number of recombined cells could be detected). The embryos were harvested and analyzed at E14.0 to E15.5. As expected,

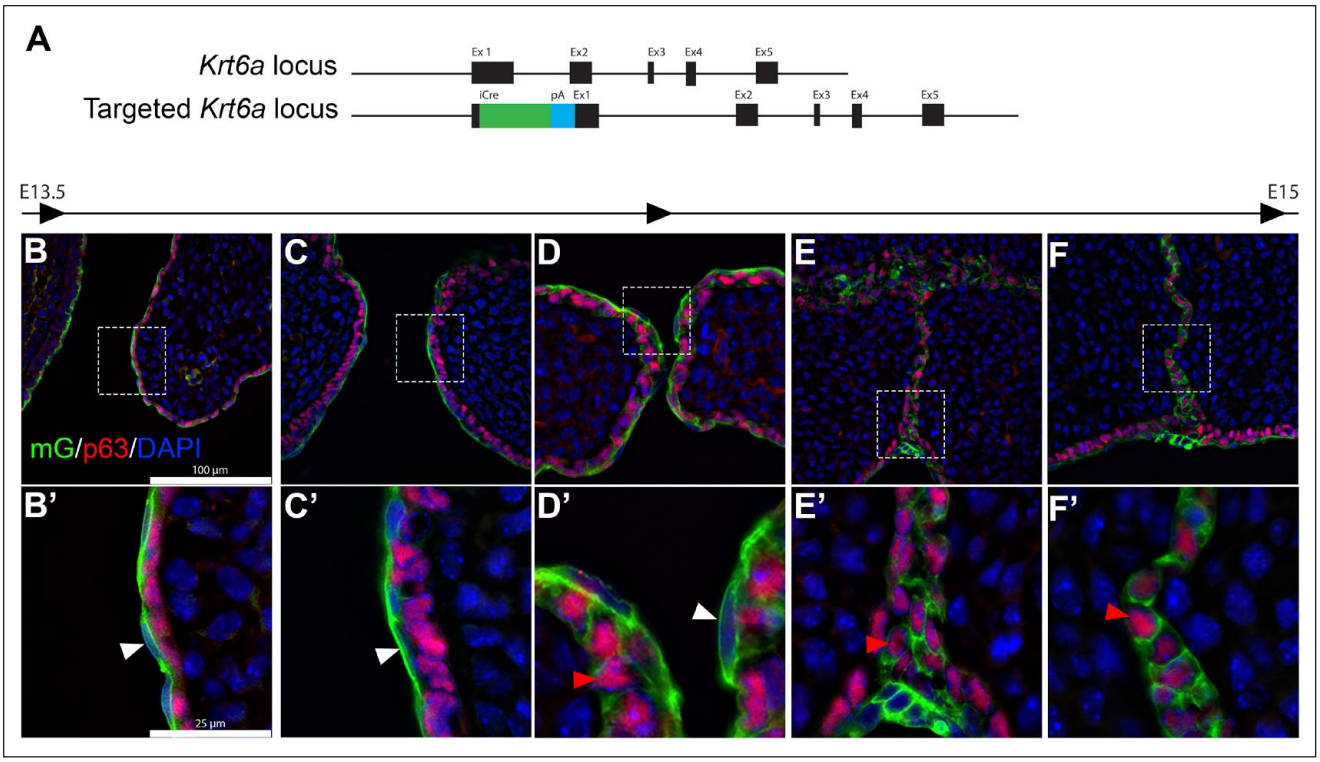

Figure 2. *Krt6iCre* induces recombination in the periderm of prefusion palatal shelves. (**A**) Schematic of the *Krt6a* genomic locus and the *Krt6aiCre*-targeted locus. Ex1, Ex2, Ex3, Ex4, and Ex5: exons 1 to 5; green box: iCre; blue box: polyadenylation (pA) sequence. (**B**) Palatal shelves (PS) before elevation (E13.5). (**C**) Palatal shelves before contact (E14.0). (**D**) Palatal shelves almost contacting (early E14.5). (**E**) Palatal shelves showing the midline seam (late E14.5). (**F**) Palatal shelves showing the fusing midline seam (E15.0). B′, C′, D′, E′, and F′ show the high-power images of the fields illustrated with hatched boxes in B, C, D, E, and F, respectively. Cells recombined with *Krt6aiCre* show membrane-bound green fluorescence. Basal epithelial cells were identified with immunostaining for p63 (red fluorescence; red arrowheads). White arrowheads mark the flattened periderm cells precontact; red arrowheads mark the p63-positive rounded green fluorescence protein (GFP)–positive cells. Counterstaining with DAPI (blue fluorescence).

in prefusion palatal shelves, the Cre-induced marker gene recombination could be detected specifically in PD cells, which displayed a characteristic flattened cell morphology (Fig. 3C). In contrast, in palatal shelves forming the contact, the PD-derived cells that showed positive marker gene recombination had lost their flattened phenotype and appeared cuboidal, like those seen in the underlying p63-positive basal epithelium (Fig. 3D, E). In samples showing the midline seam, we could detect PD-derived cuboidal GFP-positive cells, some of which also were weakly positive for the basal epithelial marker, p63 (Fig. 3F). Both the flattened and cuboidal cells recombined with *Krt6aiCre* or *Krt6aiCre*^{ERT2} stained positive for Krt14, which has generally been thought to be a basal cell marker (Athwal et al. 2019), although in the prefusion palate, it also is present in the palatal periderm (Appendix Fig. 6) (Hu et al. 2015). These data suggest that upon the palatal fusion, at least some of the palatal PD cells lose their flattened PD-like phenotype and dedifferentiate into cuboidal basal cell–like epithelial cells.

Partially Penetrant Cleft Palate Phenotype in Tgfbr1:Krt6aiCre *Mutants*

To address the role of TGF-β signaling in the PD, we crossed *Krt6aiCre* mice with mice carrying the floxed *Tgfbr1* allele. The resulting *Tgfbr1:Krt6aiCre* mutants displayed a cleft palate phenotype with a variable penetrance (Fig. 4). While some mutants showed incomplete clefts characterized with both anterior and posterior fusion defects, remarkably, a subset of *Tgfbr1::Krt6aiCre* mutants (33%, $n = 12$) displayed a complete cleft of the secondary palate (Fig. 4C and Appendix Table 1). Interestingly, the complete cleft phenotype was never seen in epithelium-specific TGF-β receptor mutants induced with *Krt14-Cre* (Dudas et al. 2006; Xu et al. 2006), which does not induce recombination in the periderm. These data indicate that TGF-β signaling specifically in the PD plays a crucial role during palatal epithelial fusion.

Periderm Cells Deficient in the Gene Encoding the TGF-β Type I Receptor Fail to Undergo Morphological Changes and Remain Periderm-Like

To compare the fate of periderm cells deficient of *Tgfbr1* to that of wild-type cells, we generated *Krt6aiCre*$^{+}$:*Tgfbr1*^{FF}::*mTmG* mice (mutants) and their *Krt6aiCre*$^{+}$:*Tgfbr1*^{FWT}:*mTmG* littermates (controls). In prefusion palatal shelves, *Krt6aiCre*-induced similar PD-specific recombination both in controls and in mutants (Fig. 5 and Appendix Fig. 7). In contrast to contacting and fusing wild-type palatal shelves, where the

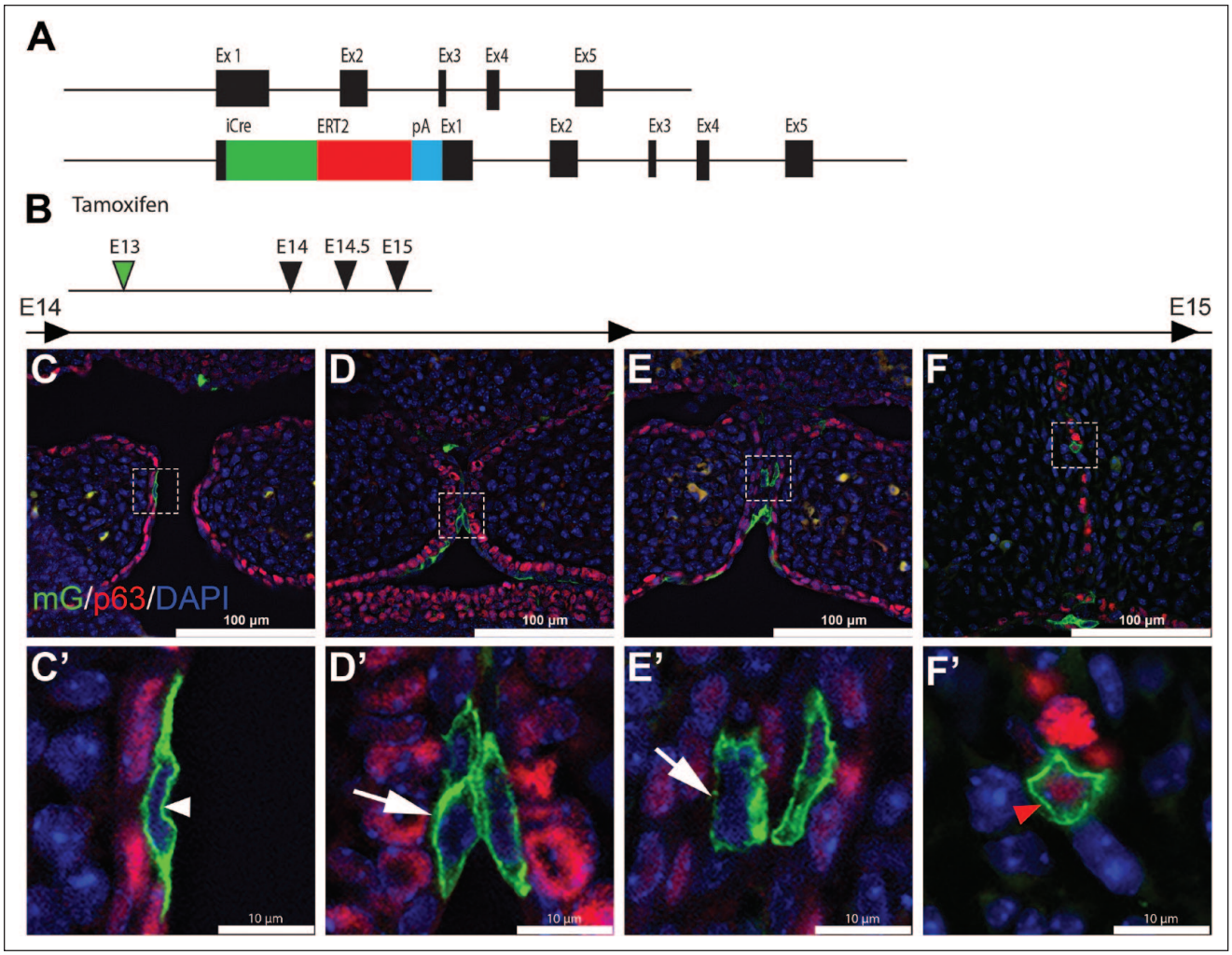

Figure 3. Lineage tracing with the *Krt6iCre*^{ERT2} mouse line reveals that upon palatal shelf contact and fusion, periderm (PD) cells dedifferentiate to cuboidal cells, which are positive for the basal cell marker, p63. (**A**) Schematic of the *Krt6a* genomic locus and the *Krt6aiCre*^{ERT2}-targeted locus. Ex1, Ex2, Ex3, Ex4, and Ex5: exons 1 to 5; green box: iCre; red box: ERT2; blue box: polyadenylation (pA) sequence. (**B**) Schematic of time of intraoral tamoxifen administration (E13: green arrow) and harvest (E14, E14.5, E15: black arrows). (**C**) Palatal shelves elevated. (**D**, **E**) Palatal shelves forming a contact. (**F**) Palatal shelves fusing showing the midline seam. C′, D′, E′, and F′ show the high-power images of the fields illustrated with hatched boxes in C, D, E, and F, respectively. Cells recombined with *Krt6aiCre*^{ERT2} show membrane-bound green fluorescence. Basal epithelial cells were identified with immunostaining for p63 (red fluorescence). White arrowhead marks the flattened periderm cell, white arrows mark the more cuboidal cells, and red arrowhead marks *Krt6aiCre*^{ERT2} recombined cell also expressing p63. Counterstaining with DAPI (blue fluorescence).

recombination could be detected in the PD-derived cells and in the underlying basal epithelial cells, in mutant littermates, the recombination remained limited to the flattened PD cells (Fig. 5). In both controls and mutants, the flattened and cuboidal recombined cells stained positive for Grhl3 and Krt17, which are proteins known to be present in the periderm (although their expression is not specific for the periderm) (Appendix Fig. 8). Quantitative analysis was performed comparing the mean nuclear length/width ratio of GFP-expressing cells among controls and mutants for both pre- and postpalatal shelf contact. There was no significant difference in mean nuclear length/width ratio between controls (mean = 3.471) and mutants (mean = 3.632) before palatal shelf contact, while mutants with postcontact palatal shelves (mean = 4.747) showed a significantly higher mean nuclear length/width ratio as compared to their control counterparts (mean = 1.920) (Fig. 5). This analysis aligns with the observation that periderm cells remain squamous before palatal shelf-contact in both controls and mutants. Furthermore, as seen by the significantly higher mean nuclear length/width ratio in mutants with postcontact palatal shelves as compared to controls, periderm cells deficient in the TGF-β type I receptor gene do not undergo a change shape and remain squamous, supporting the importance of the TGF-β type I receptor in phenotypic dedifferentiation of the periderm. These data indicate that TGF-β signaling plays a critical role specifically in the palatal PD either by

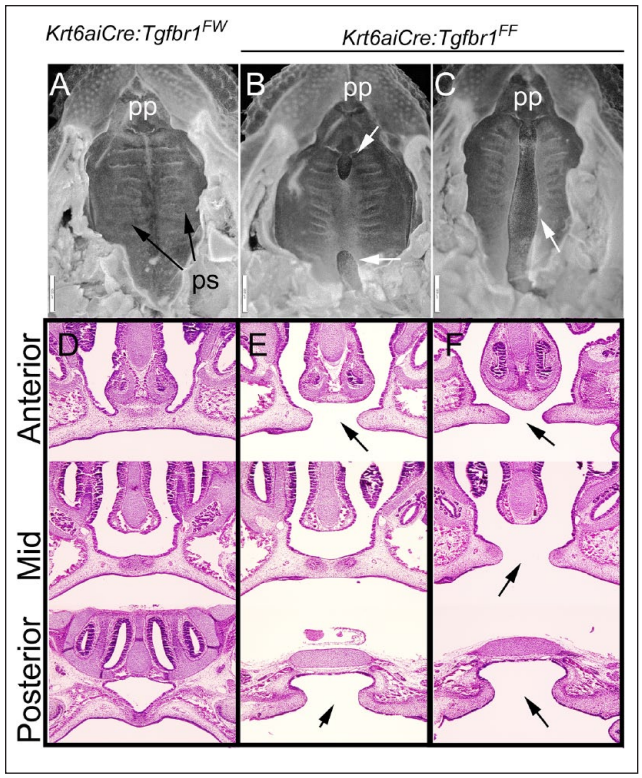

Figure 4. Deletion of transforming growth factor–β (TGF-β) type I receptor in periderm (PD) cells by the *Krt6aiCre* transgene results in cleft palate. (**A–C**) DAPI-dilactate-stained heads (mandible removed) showing the macroscopic palate phenotypes (A, control; B and C, mutants; pp, primary palate). Black arrows in A point to fused palatal shelves (ps); white arrows in B point to the anterior and posterior clefts; white arrow in C points to complete cleft. (**D–F**) Controls (D) and mutant (E, F) heads were sectioned on anterior, mid, and posterior levels. Mutant in B and E shows anterior and posterior cleft (black arrows); mutant in C and F shows complete cleft (black arrows).

permitting their phenotypic dedifferentiation (from flattened to cuboidal) or by inducing them to phenotypically dedifferentiate during palatal epithelial fusion.

Discussion

In the embryonic skin, peridermal precursors, which detach from the basement membrane and move to the surface, form a flattened "endothelial-like" *Krt-17*–positive PD cell layer in which the cells are attached to each other by tight junctions (McGowan and Coulombe 1998). Similar to the embryonic skin, *Krt-17* is also expressed in the mouse oral PD, albeit in the prefusion palatal shelves, its expression can also be seen in the basal epithelium (Jin et al. 2014) (Appendix Fig. 9) This suggests that there exist some distinct differences between the palatal oral periderm and skin periderm during mouse embryogenesis.

Recent studies have identified several genes (e.g., *Irf6*, *Grhl3*, *Ripk4*, and *Ikka*) that are required for proper PD development (Richardson et al. 2009, 2014; De Groote et al. 2015; Liu et al. 2016). Interestingly, many of these genes are direct targets of p63, the gene specifically expressed in the basal epithelium (Hammond et al. 2019). The studies examining the PD's role in palatogenesis, specifically during the palatal epithelial fusion, have been complicated by the fact that the robust and commonly used pan-epithelial *Krt14-Cre* driver (Andl et al. 2004) does not recombine in the PD (Lane, Yumoto, Pisano, et al. 2014). Thus, many studies addressing molecular and cellular regulation of palatal epithelial fusion have ignored the potential role of the PD in this process. Moreover, the lack of appropriate genetic tools has prevented a precise determination of the cellular fate of the palatal PD. Our present study suggests that some of the PD cells undergo rapid phenotypic dedifferentiation to cuboidal cells (Appendix Fig. 10). The cells recombined with the constitutive *Krt6aiCre* driver that also are positive for p63 can represent either peridermal cells that start to express p63 or basal epithelial cells that become positive for Krt6a. To resolve this issue, we generated an inducible Krt*6aiCre*^{ERT2} mouse line. Results obtained using this novel line suggest that, indeed, the p63-positive cells that have undergone tamoxifen-induced recombination are derived from the PD. Alternatively, it is still possible that the recombined cells seen in the midline seam are in fact *Krt6a*-positive cuboidal midline epithelial seam cells that have undergone late recombination. The final dissolution of the palatal midline seam composed of both the periderm-derived and the basal epithelium–derived cells takes place as previously outlined (Kim et al. 2015; Teng et al. 2022).

The critical role of TGF-β signaling for successful palatogenesis, both in the palatal epithelium and in the palatal mesenchyme, has been well documented (Ito et al. 2003; Dudas et al. 2006; Xu et al. 2006, 2008). The gene encoding TGF-β3 (*Tgfb3*) shows exceptionally strong expression in MEE cells (Fitzpatrick et al. 1990; Pelton et al. 1990), and mice deficient in *Tgfb3* show a cleft palate phenotype in which the fully grown palatal shelves fail to fuse (Kaartinen et al. 1995; Proetzel et al. 1995). Several studies have shown that p63 expression is suppressed during palatal fusion and that this suppression fails to occur in TGF-β3 and TGF-β receptor mutants (Iwata et al. 2013; Lane, Yumoto, Azhar, et al. 2014; Hu et al. 2015). Moreover, the partial rescue of the cleft palate phenotype of *Tgfb3*$^{-/-}$ mice that were heterozygotes for *p63* suggested that the key role of TGF-β3 in the MEE would be to suppress p63 expression, which would result in the periderm remodeling (Richardson et al. 2017). Our current findings show that in *Krt6aiCre:Tgfbr1* mice, periderm cells fail to dedifferentiate (Fig. 5 and Appendix Fig. 7). As a result, 33% of periderm-specific *Tgfbr1* mutant mice display a complete cleft of the secondary palate, arguing that TGF-β signaling plays a critical role specifically in the periderm. In fact, the periderm-specific role for TGF-β3 has previously been suggested by Wu et al. (2013), who injected a viral vector encoding *Tgfb3* in the amniotic fluid of *Tgfb3*$^{-/-}$ and control embryos and showed that periderm-specific transduction of *Tgfb3* was sufficient to induce palatal shelf adhesion and fusion in *Tgfb3*-deficient embryos.

In conclusion, our results suggest that the periderm cells covering prefusion palatal shelves undergo rapid phenotypic dedifferentiation during palatal epithelial fusion, which is dependent on periderm-specific TGF-β signaling. This hypothesis still needs to be tested with live imaging experiments.

Author Contributions

G. Saroya, contributed to design, data acquisition, analysis, and interpretation, drafted and critically revised the manuscript; J. Hu, contributed to design, data analysis, critically revised the manuscript; M. Hu, C. Panaretos, J. Mann, S. Kim, contributed to data analysis, critically revised the manuscript; J.O. Bush, contributed to conception, critically revised the manuscript; V. Kaartinen, contributed to conception and design, data analysis and interpretation, drafted and critically revised the manuscript. All authors gave their final approval and agreed to be accountable for all aspects of the work.

Acknowledgments

We acknowledge the Transgenic Animal Model Core of the University of Michigan's Biomedical Research Core Facilities for preparation of transgenic mice.

Declaration of Conflicting Interests

The authors declared no potential conflicts of interest with respect to the research, authorship, and/or publication of this article.

Funding

The authors disclosed receipt of the following financial support for the research, authorship, and/or publication of this article: Supported by National Institute of Child Health and Human Development and National Institute of Dental and Craniofacial Research of the National Institutes of Health under award numbers R03HD100602, R56DE026464, and R01DE013085.

ORCID iDs

G. Saroya, https://orcid.org/0000-0002-8041-9586

V. Kaartinen https://orcid.org/0000-0002-9432-510X

References

Andl T, Ahn K, Kairo A, Chu EY, Wine-Lee L, Reddy ST, Croft NJ, Cebra-Thomas JA, Metzger D, Chambon P, et al. 2004. Epithelial bmpr1a regulates differentiation and proliferation in postnatal hair follicles and is essential for tooth development. Development. 131(10):2257–2268.

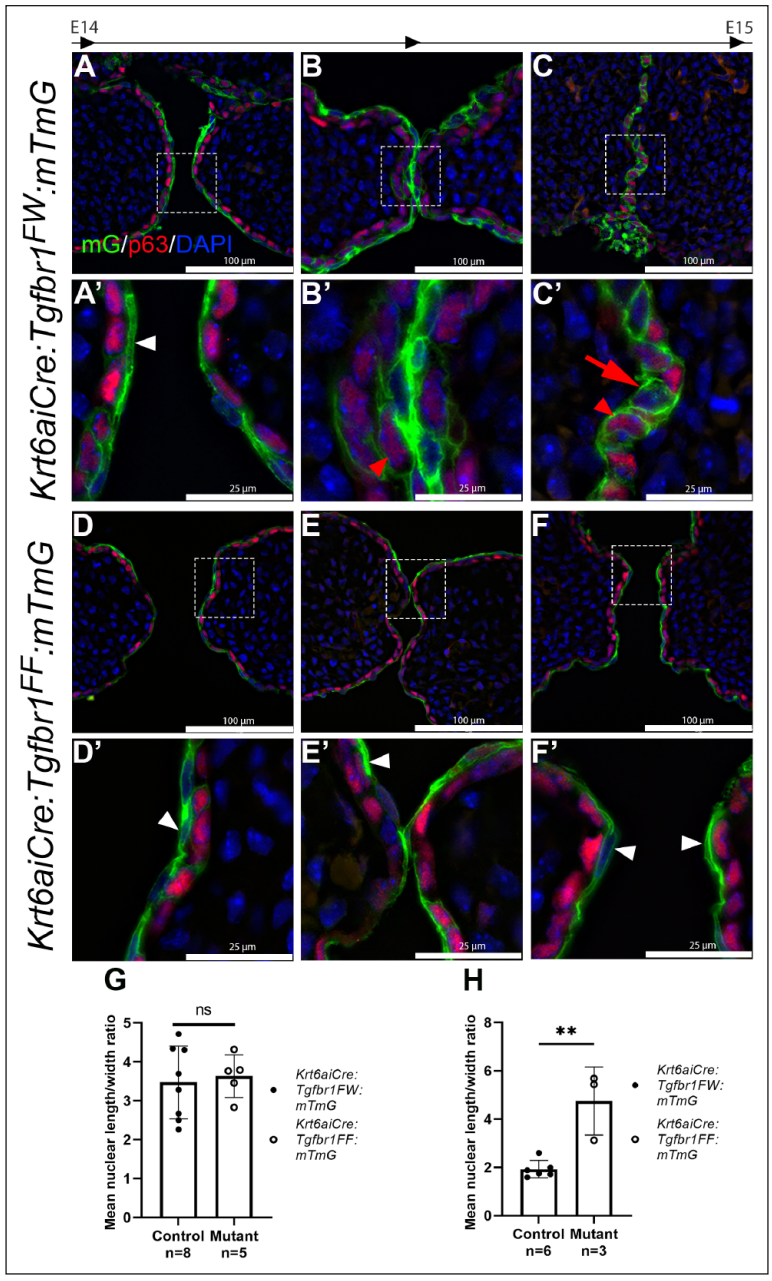

Figure 5. Periderm cells deficient in *Tgfbr1* fail to undergo morphological differentiation prior to and during the palatal shelf (PS) contact. *Krt6aiCre:Tgfbr1*^{FW}*:mTmG* controls (**A–C**) and *Krt6aiCre:Tgfbr1*^{FF}*:mTmG* mutants (**D–F**) shown at E14.0 (before PS contact), at E14.5 (PS forming a contact), and at E15.0 (PS fusing at the midline seam stage). A′, B′, C′, D′, E′, and F′ show the high-power images of the fields illustrated with hatched boxes in A to F, respectively. Cells recombined with Krt6aiCre show membrane-bound green fluorescence. Basal epithelial cells were identified with immunostaining for p63 (red fluorescence). White arrowheads mark flattened periderm cells. Red arrowheads and arrow mark *Krt6aiCre* recombined cells after palatal shelf contact with and without p63 expression, respectively. Counterstaining with DAPI (blue fluorescence). (**G**) The mean nuclear length/width ratios of green fluorescent protein (GFP)–expressing cells before PS contact between controls and mutants, $n = 8$ and $n = 5$, respectively; ns, $P = 0.7358$. (**H**) The mean nuclear length/breadth ratios of GFP-expressing cells after PS contact between controls and mutants, $n = 6$ and $n = 3$, respectively. $^{**}P = 0.0017$.

Athwal HK, Murphy G, Tibbs E, Cornett A, Hill E, Yeoh K, Berenstein E, Hoffman MP, Lombaert IMA. 2019. Sox10 regulates plasticity of epithelial progenitors toward secretory units of exocrine glands. Stem Cell Rep. 12(2):366–380.

Bush JO, Jiang R. 2012. Palatogenesis: morphogenetic and molecular mechanisms of secondary palate development. Development. 139(2):231–243.

Chai Y, Jiang X, Ito Y, Bringas P Jr, Han J, Rowitch DH, Soriano P, McMahon AP, Sucov HM. 2000. Fate of the mammalian cranial neural crest during tooth and mandibular morphogenesis. Development. 127(8):1671–1679.

Cuervo R, Covarrubias L. 2004. Death is the major fate of medial edge epithelial cells and the cause of basal lamina degradation during palatogenesis. Development. 131(1):15–24.

De Groote P, Tran HT, Fransen M, Tanghe G, Urwyler C, De Craene B, Leurs K, Gilbert B, Van Imschoot G, De Rycke R, et al. 2015. A novel ripk4-irf6 connection is required to prevent epithelial fusions characteristic for popliteal pterygium syndromes. Cell Death Differ. 22(6):1012–1024.

Dudas M, Kim J, Li WY, Nagy A, Larsson J, Karlsson S, Chai Y, Kaartinen V. 2006. Epithelial and ectomesenchymal role of the type I TGF-beta receptor alk5 during facial morphogenesis and palatal fusion. Dev Biol. 296(2):298–314.

Fitzpatrick DR, Denhez F, Kondaiah P, Akhurst RJ. 1990. Differential expression of TGF beta isoforms in murine palatogenesis. Development. 109(3):585–595.

Hammond NL, Dixon J, Dixon MJ. 2019. Periderm: life-cycle and function during orofacial and epidermal development. Semin Cell Dev Biol. 91:75–83.

Hu L, Liu J, Li Z, Ozturk F, Gurumurthy C, Romano RA, Sinha S, Nawshad A. 2015. Tgfbeta3 regulates periderm removal through deltanp63 in the developing palate. J Cell Physiol. 230(6):1212–1225.

Ito Y, Yeo JY, Chytil A, Han J, Bringas P Jr, Nakajima A, Shuler CF, Moses HL, Chai Y. 2003. Conditional inactivation of tgfbr2 in cranial neural crest causes cleft palate and calvaria defects. Development. 130(21):5269–5280.

Iwata J, Suzuki A, Pelikan RC, Ho TV, Sanchez-Lara PA, Urata M, Dixon MJ, Chai Y. 2013. Smad4-Irf6 genetic interaction and TGFbeta-mediated irf6 signaling cascade are crucial for palatal fusion in mice. Development. 140(6):1220–1230.

Jin JZ, Warner DR, Lu Q, Pisano MM, Greene RM, Ding J. 2014. Deciphering TGF-beta3 function in medial edge epithelium specification and fusion during mouse secondary palate development. Dev Dyn. 243(12):1536–1543.

Jugessur A, Lie RT, Wilcox AJ, Murray JC, Taylor JA, Saugstad OD, Vindenes HA, Abyholm F. 2003. Variants of developmental genes (tgfa, tgfb3, and msx1) and their associations with orofacial clefts: a case-parent triad analysis. Genet Epidemiol. 24(3):230–239.

Kaartinen V, Voncken JW, Shuler C, Warburton D, Bu D, Heisterkamp N, Groffen J. 1995. Abnormal lung development and cleft palate in mice lacking TGF-beta 3 indicates defects of epithelial-mesenchymal interaction. Nat Genet. 11(4):415–421.

Kim S, Lewis AE, Singh V, Ma X, Adelstein R, Bush JO. 2015. Convergence and extrusion are required for normal fusion of the mammalian secondary palate. PLoS Biol. 13(4):e1002122.

Lan Y, Wang Q, Ovitt CE, Jiang R. 2007. A unique mouse strain expressing cre recombinase for tissue-specific analysis of gene function in palate and kidney development. Genesis. 45(10):618–624.

Lan Y, Xu J, Jiang R. 2015. Cellular and molecular mechanisms of palatogenesis. Curr Top Dev Biol. 115:59–84.

Lane J, Kaartinen V. 2014. Signaling networks in palate development. Wiley Interdiscip Rev Syst Biol Med. 6(3):271–278.

Lane J, Yumoto K, Azhar M, Ninomiya-Tsuji J, Inagaki M, Kim J, Mishina Y, Kaartinen V. 2014. Tak1, smad4 and trim33 redundantly mediate TGF-β3 signaling during palate development. Dev Biol. 398(2):231–241.

Lane J, Yumoto K, Pisano J, Azhar M, Thomas PS, Kaartinen V. 2014. Control elements targeting tgfb3 expression to the palatal epithelium are located intergenically and in introns of the upstream ift43 gene. Front Physiol. 5:258.

Lidral AC, Romitti PA, Basart AM, Doetschman T, Leysens NJ, Daack-Hirsch S, Semina EV, Johnson LR, Machida J, Burds A, et al. 1998. Association of msx1 and tgfb3 with nonsyndromic clefting in humans. Am J Hum Genet. 63(2):557–568.

Liu H, Leslie EJ, Jia Z, Smith T, Eshete M, Butali A, Dunnwald M, Murray J, Cornell RA. 2016. Irf6 directly regulates klf17 in zebrafish periderm and klf4 in murine oral epithelium, and dominant-negative klf4 variants are present in patients with cleft lip and palate. Hum Mol Genet. 25(4):766–776.

Liu HX, Komatsu Y, Mishina Y, Mistretta CM. 2012. Neural crest contribution to lingual mesenchyme, epithelium and developing taste papillae and taste buds. Dev Biol. 368(2):294–303.

McGowan KM, Coulombe PA. 1998. Onset of keratin 17 expression coincides with the definition of major epithelial lineages during skin development. J Cell Biol. 143(2):469–486.

Parada C, Li J, Iwata J, Suzuki A, Chai Y. 2013. Ctgf mediates smad-dependent TGFbeta signaling to regulate mesenchymal cell proliferation during palate development. Mol Cell Biol. 33(17):3482–3493.

Pelton RW, Hogan BL, Miller DA, Moses HL. 1990. Differential expression of genes encoding TGFs beta 1, beta 2, and beta 3 during murine palate formation. Dev Biol. 141(2):456–460.

Proetzel G, Pawlowski SA, Wiles MV, Yin M, Boivin GP, Howles PN, Ding J, Ferguson MW, Doetschman T. 1995. Transforming growth factor-beta 3 is required for secondary palate fusion. Nat Genet. 11(4):409–414.

Richardson R, Mitchell K, Hammond NL, Mollo MR, Kouwenhoven EN, Wyatt ND, Donaldson IJ, Zeef L, Burgis T, Blance R, et al. 2017. P63 exerts spatio-temporal control of palatal epithelial cell fate to prevent cleft palate. PLoS Genet. 13(6):e1006828.

Richardson RJ, Dixon J, Jiang R, Dixon MJ. 2009. Integration of irf6 and jagged2 signalling is essential for controlling palatal adhesion and fusion competence. Hum Mol Genet. 18(14):2632–2642.

Richardson RJ, Hammond NL, Coulombe PA, Saloranta C, Nousiainen HO, Salonen R, Berry A, Hanley N, Headon D, Karikoski R, et al. 2014. Periderm prevents pathological epithelial adhesions during embryogenesis. J Clin Invest. 124(9):3891–3900.

Sandell L, Inman K, Trainor P. 2018. DAPI staining of whole-mount mouse embryos or fetal organs. Cold Spring Harb Protoc. 2018(10). doi:10.1101/pdb.prot094029

Teng T, Teng CS, Kaartinen V, Bush JO. 2022. A unique form of collective epithelial migration is crucial for tissue fusion in the secondary palate and can overcome loss of epithelial apoptosis. Development. 149(10):dev200181.

Vieira AR, Orioli IM, Castilla EE, Cooper ME, Marazita ML, Murray JC. 2003. Msx1 and tgfb3 contribute to clefting in South America. J Dent Res. 82(4):289–292.

Wu C, Endo M, Yang BH, Radecki MA, Davis PF, Zoltick PW, Spivak RM, Flake AW, Kirschner RE, Nah HD. 2013. Intra-amniotic transient transduction of the periderm with a viral vector encoding tgfbeta3 prevents cleft palate in tgfbeta3$^{-/-}$ mouse embryos. Mol Ther. 21(1):8–17.

Xu X, Han J, Ito Y, Bringas P Jr, Deng C, Chai Y. 2008. Ectodermal smad4 and p38 MAPK are functionally redundant in mediating TGF-beta/BMP signaling during tooth and palate development. Dev Cell. 15(2):322–329.

Xu X, Han J, Ito Y, Bringas P Jr, Urata MM, Chai Y. 2006. Cell autonomous requirement for tgfbr2 in the disappearance of medial edge epithelium during palatal fusion. Dev Biol. 297(1):238–248.

Yoshida M, Shimono Y, Togashi H, Matsuzaki K, Miyoshi J, Mizoguchi A, Komori T, Takai Y. 2012. Periderm cells covering palatal shelves have tight junctions and their desquamation reduces the polarity of palatal shelf epithelial cells in palatogenesis. Genes Cells. 17(6):455–472.